

Digital subcarrier multiplexing for flexible spectral allocation in optical transport network

Yuanyuan Zhang,¹ Maurice O'Sullivan,² and Rongqing Hui^{1,*}

¹Dept. Electrical Eng. & Computer Science, The University of Kansas, Lawrence, Kansas 66045, USA

²Ciena, Ottawa Carling Campus, 3500 Carling Ave., Nepean, ON, K2H 8E9, Canada

*rhui@ku.edu

Abstract: We demonstrate a spectrally efficient digital subcarrier multiplexed (DSCM) coherent optical system for optical transport network. In the proposed system, mutually orthogonal subcarrier channels are digitally generated, which allows a high degree of flexibility in bandwidth allocation and scalability in data rate granularity. The receiver can also dynamically change the number of DSCM channels for detection without changing the system configuration. We experimentally investigate the transmission performance of a 22.2Gb/s DSCM system with 10 subcarrier channels using QPSK modulation. The impacts of channel spacing and time mismatch between subcarrier channels are also explored.

©2011 Optical Society of America

OCIS codes: (060.0060) Fiber Optics and optical communications; (250.0250) Optoelectronics.

References and links

1. S. J. B. Yoo, "Optical packet and burst switching technologies for the future photonic Internet," *J. Lightwave Technol.* **24**(12), 4468–4492 (2006).
2. M. Tomizawa, J. Yamawaku, Y. Takigawa, M. Koga, Y. Miyamoto, T. Morioka, and K. Hagimoto, "Terabit LAN with optical virtual concatenation for Grid applications with super-computers," in *Optical Fiber Communication Conference (OFC)*, 2005), OThG6.
3. X. J. Cao, V. Anand, and C. M. Qiao, "Waveband switching in optical networks," *IEEE Commun. Mag.* **41**(4), 105–112 (2003).
4. M. Jinno, H. Takara, B. Kozicki, Y. Tsukishima, Y. Sone, and S. Matsuoka, "Spectrum-Efficient and Scalable Elastic Optical Path Network: Architecture, Benefits, and Enabling Technologies," *IEEE Commun. Mag.* **47**(11), 66–73 (2009).
5. K. Christodoulopoulos, I. Tomkos, and E. A. Varvarigos, "Elastic Bandwidth Allocation in Flexible OFDM-Based Optical Networks," *J. Lightwave Technol.* **29**(9), 1354–1366 (2011).
6. A. J. Lowery and J. Armstrong, "Orthogonal-frequency-division multiplexing for dispersion compensation of long-haul optical systems," *Opt. Express* **14**(6), 2079–2084 (2006).
7. A. F. Molisch, *Wireless Communications* (Wiley, 2011).
8. T. Kobayashi, A. Sano, E. Yamada, E. Yoshida, and Y. Miyamoto, "Over 100 Gb/s Electro-Optically Multiplexed OFDM for High-Capacity Optical Transport Network," *J. Lightwave Technol.* **27**(16), 3714–3720 (2009).
9. B. Kozicki, H. Takara, Y. Tsukishima, T. Yoshimatsu, K. Yonenaga, and M. Jinno, "Experimental demonstration of spectrum-sliced elastic optical path network (SLICE)," *Opt. Express* **18**(21), 22105–22118 (2010).
10. Y. Y. Zhang, M. O'Sullivan, and R. Q. Hui, "Theoretical and experimental investigation of compatible SSB modulation for single channel long-distance optical OFDM transmission," *Opt. Express* **18**(16), 16751–16764 (2010).
11. K. Roberts, C. Li, L. Strawczynski, M. O'Sullivan, and I. Hardcastle, "Electronic pre-compensation of optical nonlinearity," *IEEE Photon. Technol. Lett.* **18**(2), 403–405 (2006).
12. Y. R. Ma, Q. Yang, Y. Tang, S. M. Chen, and W. Shieh, "1-Tb/s single-channel coherent optical OFDM transmission over 600-km SSMF fiber with subwavelength bandwidth access," *Opt. Express* **17**(11), 9421–9427 (2009).
13. W. Shieh, H. Bao, and Y. Tang, "Coherent optical OFDM: theory and design," *Opt. Express* **16**(2), 841–859 (2008).
14. A. J. Viterbi and A. M. Viterbi, "Non-linear estimation of PSK-modulated carrier phase with application to burst digital transmission," *IEEE Trans. Inf. Theory* **29**(4), 543–551 (1983).
15. R. Q. Hui, B. Y. Zhu, R. X. Huang, C. T. Allen, K. R. Demarest, and D. Richards, "Subcarrier multiplexing for high-speed optical transmission," *J. Lightwave Technol.* **20**(3), 417–427 (2002).
16. G. Bosco, A. Carena, V. Curri, P. Poggiolini, and F. Forghieri, "Performance Limits of Nyquist-WDM and CO-OFDM in High-Speed PM-QPSK Systems," *IEEE Photon. Technol. Lett.* **22**(15), 1129–1131 (2010).
17. S. Chandrasekhar and X. Liu, "Experimental investigation on the performance of closely spaced multi-carrier

- PDM-QPSK with digital coherent detection,” *Opt. Express* **17**(24), 21350–21361 (2009).
18. X. Liu, X. Wei, S. Chandrasekhar, and A. H. Gnauck, “Increased OSNR gains of forward-error correction in nonlinear optical transmissions,” *IEEE Photon. Technol. Lett.* **15**(7), 999–1001 (2003).
-

1. Introduction

High speed bandwidth scalable transmission systems are under consideration as a means of addressing flexible capacity requirements of next generation optical networks. Wavelength routed transparent network architectures can reduce the need for electrical regeneration, and by this reduce network cost. For optical switching and grooming on shorter timescales several approaches have been proposed in recent years, namely, optical packet switching (OPS) [1], optical virtual concatenation (OVC) [2], and waveband switching [3]. The enabling technologies such as fast optical switches and optical buffers are still in gestation. The spectrum-sliced elastic optical path network (SLICE) is a demonstrated alternative network architecture [4] with improved bandwidth granularity in comparison to present WDM-based and wavelength-routed optical path networks. As one of the most important enabling technologies, bandwidth-variable transponders have gained considerable attention recently [5]. Orthogonal frequency division multiplexing (OFDM) is a very promising candidate, since it provides variable bandwidth allocation by selecting the number of assigned subcarriers according to traffic volume and granularity requirement, yet eliminates the requirement for a spectral guard-band between adjacent subcarrier channels.

Originated from wireless communication, in a traditional FFT-based OFDM system, the data stream is first mapped into a 2-D array in the row-by-row manner, whereas an IFFT is performed such that each column of the data array becomes a subcarrier channel. In this way an OFDM symbol is usually partitioned into different subcarriers [6]. In the corresponding OFDM receiver, an FFT process is used to convert the 2-D data array back into frequency domain and the original digital signal is reconstructed through parallel to serial conversion. In addition to the extra computational complexity due to IFFT and FFT, in this process, it is not practical to select a subset of subcarriers without detecting the entire OFDM frame. In addition, the FFT-based OFDM requires pilot subcarriers and temporal guard interval for carrier recovery and synchronization [6], which increases the frame overhead. The combined overhead due to the guard interval and pilot subcarriers in FFT-based OFDM is typically 25% of total bits [7]. This reduces the bandwidth efficiency of FFT-based OFDM.

Wavelength-domain OFDM system described in [8] and [9] applies the orthogonality principle to multi wavelength systems so that the spectral guard band between WDM channels is not required. A wavelength-domain OFDM system uses mutually frequency-locked optical subcarriers created by a multicarrier comb generator, and an array of electro-optic modulators are used to encode data signals onto these optical carriers. In this scheme, channel spacing is determined by the multicarrier generator, and data rate on each wavelength channel cannot be dynamically changed without sacrificing optical bandwidth efficiency. This reduces the flexibility in bandwidth allocation as well as data rate granularity in the optical network.

In this paper, we investigate the performance of a digital subcarrier multiplexed (DSCM) system with flexible bandwidth assignment in the transmitter and dynamic channel selectivity at the receiver. In a DSCM system, subcarrier channels are digitally generated and linearly up-converted to an optical carrier by an electro-optic IQ modulator. This allows a higher degree of flexibility in bandwidth allocation and scalability in data rate granularity while maintaining high bandwidth efficiency. The receiver with coherent detection has the flexibility to dynamically select different number of DSCM channels in the detection without the need to change system configuration. The bandwidth requirement in the receiver should be reduced if only a subset of subcarrier channels is to be detected instead of the entire OFDM frame. We experimentally demonstrate a 22.2Gb/s DSCM system with 10 subcarrier channels using QPSK modulation based on a commercially available transmitter card which was originally designed for 10 Gb/s binary optical transmission with electrical-domain pre-compensation (eDCO) [10, 11]. The impact of inter-channel crosstalk and tolerance to bit

misalignment are discussed. Numerical simulations are performed to understand various mechanisms which determine system transmission performance.

2. Flexible bandwidth allocation

Wavelength-domain OFDM system has been studied as the bandwidth variable transponder for SLICE [9]. In that system, mutually frequency-locked optical carriers were generated through a comb generator [12]. These carriers were optically demultiplexed so that each could be modulated by an independent electro-optic modulator before recombined and launched into a transmission fiber. The clock of the data signal driving each modulator is synchronized to satisfy the orthogonality condition of OFDM. Practically, 10Gb/s, 40Gb/s and 100Gb/s data rates carried by each optical carrier have been demonstrated, and the aggregated data rate can reach terabits per second in such a wavelength-domain OFDM system [13]. However, from network application point of view, a finer channel data rate granularity is desired to improve network flexibility and reduce blocking probability [5]. Realistically it is not efficient to generate optical frequency combs with very narrow channel spacing (e.g., 1GHz). Also, it is not efficient for using a large number of electro-optic modulators with each only operating at a low data rate.

In order to improve data rate granularity and simplify the transmitter implementation, a DSCM modulation format can be used in which subcarriers are generated digitally in the electronics domain. Since all subcarrier channels share the same wideband electro-optic modulator, bandwidth allocation and data rate granularity can be digitally adjusted without changing transmitter optical configuration. In comparison to subcarrier generation using optical techniques, digital signal processing (DSP) in electrical domain can provide better reliability and flexibility. Technological advances in high-speed digital-to-analog converters (DAC) and modulation formats with high spectrum efficiency in recent years have made the DSCM transmitter practical. It is also straightforward to combine DSCM technique with wavelength-domain OFDM [8, 9] to provide both high data rate throughput and flexible data rate granularity.

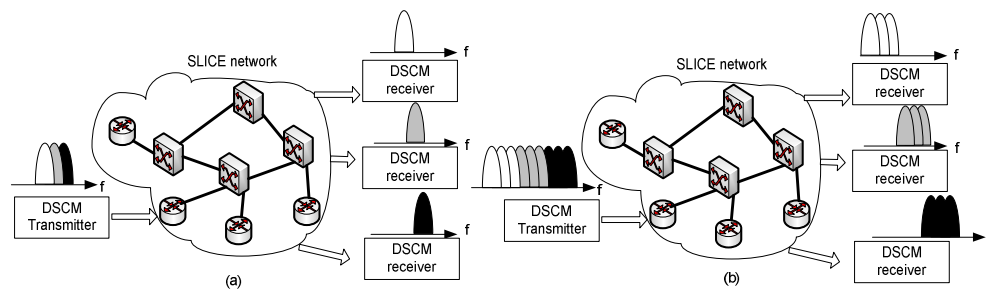


Fig. 1. SLICE transponder using DSCM.

As illustrated in Fig. 1 (a), the lowest data rate that can be assigned to each end user is that assigned on each subcarrier. Whereas, multiple subcarriers may also be dedicated to an end user if higher data rate is required in SLICE (Fig. 1 (b)). In the wavelength-domain OFDM system proposed in [9], each subcarrier channel requires a standard receiver. The implementation may become expensive as the number of subcarriers increases although the data rate per channel may be low, and the structure is not flexible for dynamic bandwidth allocation. In the DSCM system, by using coherent detection, DSP in the receiver allows the flexible selection of any subcarrier channels within the receiver bandwidth, and these subcarriers do not have to be adjacent to each other, as will be detailed in section 4.

3. Experimental setup

In order to experimentally investigate the DSCM system, we have assembled a test-bed which is schematically shown in Fig. 2. Parallel data streams are digitally modulated onto different

subcarriers in a DSP, and then the in-phase and quadrature components are converted from digital to analog format by an arbitrary waveform generator composed of two 22.2GS/s, 6-bits DACs. The analog voltage waveforms are amplified to drive an optical IQ modulator. The overall analog bandwidth of the transmitter is approximately 10GHz. At the output of the modulator, an erbium-doped fiber amplifier (EDFA) is used to boost the optical signal power to approximately 1dBm before it is launched into 75km standard single mode fiber for transmission. For these experiments the same (100 KHz linewidth) laser was used as both the light source in the transmitter and the local oscillator in the coherent receiver. Local oscillator tuning with respect to the transmitted frequency was accomplished with a sinusoid modulation of a Mach-zehnder intensity modulator biased at the minimum transmission point. In this way the optical carrier was suppressed and two narrow sidebands were generated in the optical spectrum at the modulation frequency as shown in inset (b) of Fig. 1. An FBG optical filter with a 3dB bandwidth of 0.08nm was used to reject one of the two sidebands (insertion (c) in Fig. 1). In the coherent intradyne receiver, the local oscillator is combined with the received optical signal in a 2x2 fiber-optic 90 degree hybrid so that the in-phase and the quadrature components from the received optical signal can be independently recovered after photodetection. The RF bandwidths are 32GHz for the photodiodes and 37GHz for the RF pre-amplifiers. The electrical signals are then sampled and recorded by a real-time oscilloscope (LeCroy 8600A) which has 20GS/s ADC sampling rate and approximately 6 GHz analog bandwidth. Receiver signal processing functions, including synchronization, subcarrier separation and carrier recovery are performed offline in a MATLAB program.

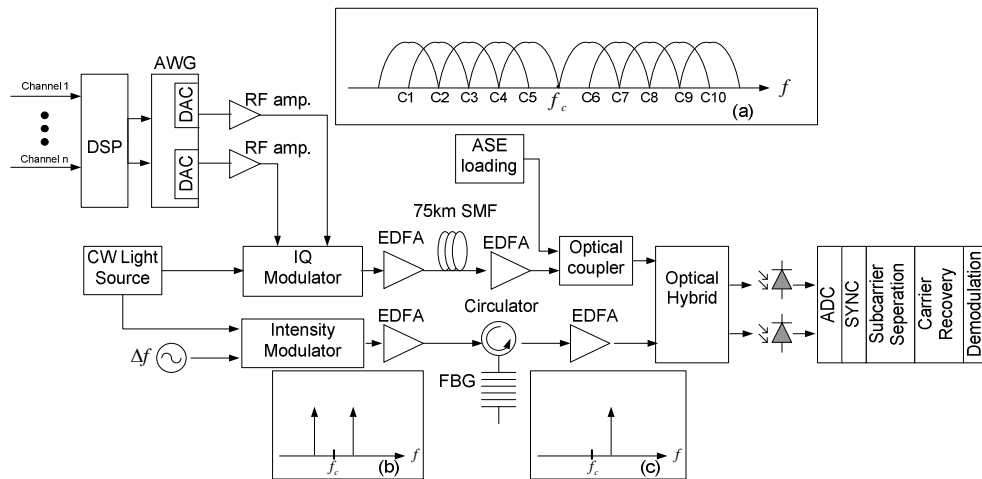


Fig. 2. System setup block diagram.

To measure the system transmission performance, an adjustable amount of ASE noise is added to the optical signal before the coherent receiver and the required optical signal to noise ratio (R-OSNR) to achieve the target bit error rate (BER) is evaluated. In fact, in an optical system with multiple subcarriers, the signal optical power is divided into subcarrier channels, and therefore the performance is determined primarily by the required optical carrier to noise ratio (R-OCNR), which is defined as the power ratio between signal power of each subcarrier and the optical noise within 0.1nm resolution bandwidth.

For the data mapping in DSP, we first generate ten parallel data streams, with each consisting of digitally modulated symbols. Each data stream is directly uploaded onto a subcarrier frequency and multiplexed with other subcarriers to form a composite OFDM signal. The two parallel voltage waveforms used to drive the two arms of the IQ modulator can be derived based on [8]:

$$S_I(t) = \sum_{k=1}^m \{Q_{kL}(t) - Q_{kU}(t)\} \cos\left(2\pi \frac{\Delta f \cdot k}{2}\right) + \sum_{k=1}^m \{I_{kU}(t) - I_{kL}(t)\} \sin\left(2\pi \frac{\Delta f \cdot k}{2}\right) \quad (1)$$

$$S_Q(t) = \sum_{k=1}^m \{I_{kL}(t) + I_{kU}(t)\} \cos\left(2\pi \frac{\Delta f \cdot k}{2}\right) + \sum_{k=1}^m \{Q_{kU}(t) + Q_{kL}(t)\} \sin\left(2\pi \frac{\Delta f \cdot k}{2}\right) \quad (2)$$

Where I_{kU} and Q_{kU} are in-phase and quadrature components of the k -th subcarrier in the upper side frequency band of the optical carrier (e.g. C6, C7, C8, C9 and C10 in inset (a) of Fig. 1); similarly, I_{kL} and Q_{kL} are in-phase and quadrature components of the k -th subcarrier in the lower side frequency band of the optical carrier (e.g. C1, C2, C3, C4 and C5 in inset (a) of Fig. 1); and Δf represents the bandwidth of each subcarrier. In the experiment, we have applied QPSK modulation on each subcarrier with 2.22Gb/s data rate. A total of 10 subcarrier channels were used, with 5 on each side of the optical carrier and the subcarrier channel spacing was 1.11GHz. The optical bandwidth efficiency was approximately 2b/Hz.

In the receiver, the off-line signal processing included inter-channel crosstalk rejection, carrier recovery and time synchronization. To prepare the data for signal recovery, data of both the I and the Q channels downloaded from the oscilloscope were re-sampled to 20 samples per bit by interpolation, DC component was removed and the amplitude was re-normalized. The inter-channel crosstalk rejection was done by digital integration through a 19-tap finite-impulse-response (FIR) filter with 50 picosecond delay time. Time synchronization was performed by pilot bits. After synchronization, data was sliced to one sample per bit. Carrier recovery was accomplished with Viterbi-and-Viterbi phase estimation (VVPE) [14], in which samples went through an M^{th} power operation (M is the modulation level, with $M = 4$ for the QPSK system) to remove the modulation. The average phase estimation was obtained from an 11-tap FIR filter, and finally the phase of the samples was corrected according to the unwrapped phase estimation.

4. Results and discussion

4.1 DSCM optical spectra

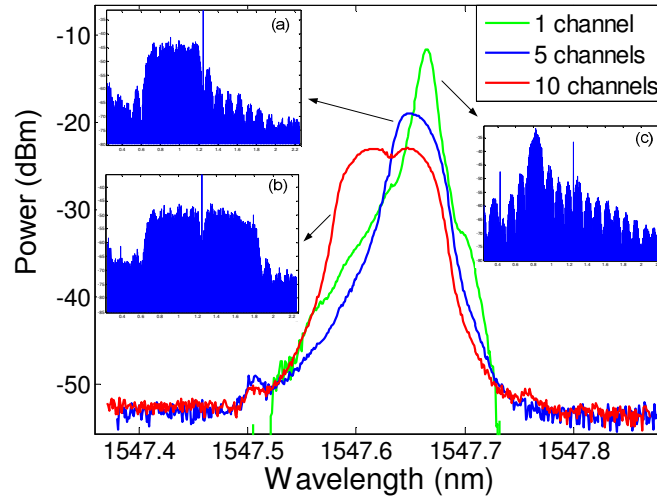


Fig. 3. Optical spectra of QPSK modulation systems.

One of the advantages of coherent detection is the better utilization of optical bandwidth in comparison to direct detection. In the optical transmitter, an IQ modulator allows independent data signals to be loaded onto the upper and the lower optical sidebands without interaction. The IQ modulator consists of a Mach-zehnder interferometer with an intensity modulator in

each arm, and a phase shifter between the two arms. In order to suppress the optical carrier, both of the two intensity modulators should be biased at the minimum power transmission point. While the phase shifter has to be biased at the quadrature point which allows the in-phase and the quadrature components to be mapped into the upper and the lower optical sidebands. Figure 3 shows the measured optical spectra using an optical spectrum analyzer with a 0.01nm resolution bandwidth. The insets in Fig. 3 show the corresponding electrical spectra measured by a coherent heterodyne detection and an RF spectrum analyzer to provide a better spectral resolution. Figure 3 indicates that when data is loaded onto subcarrier channels on one side of the optical carrier, the power leaked into the opposite sideband of the carrier ranges approximately from -15dB to -20dB . This single sideband (SSB) power suppression ratio determines the level of crosstalk between the two optical sidebands when both of them are loaded with data. Note that crosstalk between channels on the opposite sides of the optical carrier due to the non ideal SSB power suppression has different nature compared to that between mutually orthogonal subcarrier channels. The impact of this crosstalk as illustrated in insets (a) and (b) in Fig. 3 cannot be removed by integration over 1-symbol period because the power leaked from the opposite sideband has the same spectral component as the signal channel. Precise bias control of the phase shifter in the IQ modulator is essential for minimizing the crosstalk between the upper and the lower optical sidebands.

4.2 Experiment results and discussion

Thanks to the flexibility of DSP and I/Q modulation in the transmitter, and digital phase recovery in the coherent receiver, multi-level modulation can be used which utilizes both amplitude and phase information of the optical signal. In this section, we discuss DSCM system with QPSK modulation in each subcarrier.

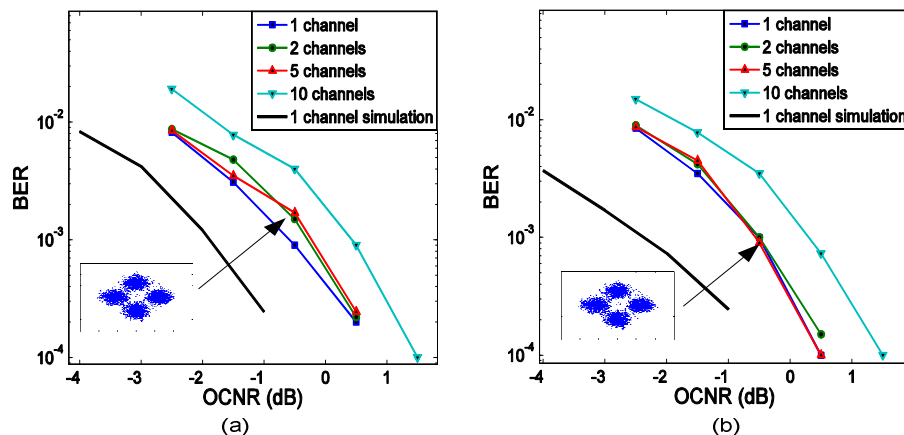


Fig. 4. Measured BER vs. OCNR in QPSK system: (a) back-to-back; (b) after 75km SMF.

Figure 4 shows the measured BER vs. OCNR with different number of channels. There is negligible increase in OCNR penalty when the number of subcarrier channels increases from 1 to 5. Note that in these measurements, all the 5 subcarrier channels are located on the upper sideband with respect to the center optical carrier. When the other 5 subcarrier channels on the lower sideband of the spectrum are added to make the total channel count to be 10, there is an approximately 1 dB OCNR penalty introduced. This can be partly attributed to the imperfect sideband suppression in the SSB modulation process as described in section 4.1. Compare Fig. 4 (b) with Fig. 4 (a), there is negligible OCNR degradation introduced by 75km transmission fiber. Results of numerical simulation are also shown in Fig. 4. In the simulation the linewidth of the laser was 100kHz, the fiber dispersion was $D = 16 \times 10^{-6} \text{ s/m}^2$, nonlinear index was $n_2 = 2.6 \times 10^{-20} \text{ m}^2/\text{W}$, and the attenuation was $\alpha = 0.2\text{dB/km}$. The sampling rate

of DAC and ADC were both 22.2GS/s, and other components were considered ideal with infinite bandwidths. A 1nm optical filter was used in front of the photodetector and a 6GHz electrical filter after the photodetector to simulate the bandwidth limit of the oscilloscope in the experiment. For a single channel system, simulation predicted an approximately 1.5dB lower R-OCNR compared to the experiment for the BER of 10^{-3} . We attribute this discrepancy to the distortion introduced by pass band ripple in RF amplifiers, multiple reflections in the RF and optical paths, as well as time jitter in the ADC process. For an ideal system only considering local oscillator-ASE beat noise in the coherent detection, an oversimplified analytical solution can be obtained as $OSNR = Q^2 B_e / (2B_0)$ which provides the ultimate OSNR requirement for the QPSK system. For the optical bandwidth $B_0 = 12.5\text{GHz}$ (0.1nm) used to measure OSNR and electrical bandwidth $B_e = 1.11\text{GHz}$ (for 2.22GHz QPSK data rate), the required OSNR for $Q = 3.08$ ($\text{BER} \approx 10^{-3}$) should be -3.75dB .

In a multi-carrier system, channel orthogonality is determined by the ratio between the symbol rate and the channel spacing. Ideally in an OFDM system with rectangular data pulses, digital integration over one symbol period is able to remove the inter-channel crosstalk [7]. However, if the bandwidth of the system is not much wider than that of a subcarrier, crosstalk cancellation may not be complete, depending on the actual shape of the pulses. Practically in high data rate wavelength-domain OFDM, the component bandwidth may only be comparable to the symbol rate per subcarrier, and the residual inter-channel crosstalk may be significant.

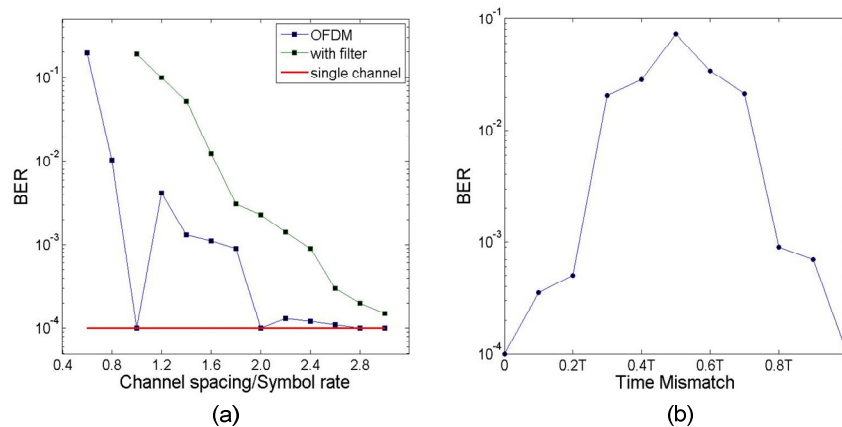


Fig. 5. (a) Measured BER vs. normalized channel spacing in QPSK system, and (b) Measured BER vs. time mismatch

To demonstrate the orthogonality between adjacent subcarrier channels and the cancellation of inter-channel crosstalk through signal processing, Fig. 5(a) shows the measured BER as a function of normalized channel spacing between adjacent subcarrier channels. In this experiment, two subcarrier channels were transmitted over 75km standard single-mode fiber (SMF), and the BER was measured with 1dB OCNR at the receiver. In this DSCM system, the receiver bandwidth is approximately 6GHz, which is much wider than that of each subcarrier channel, and therefore BER degradation can be eliminated through digital integration when the channel spacing is integer multiple of the symbol rate. On the other hand, if a simple 5th order Bessel filter is used with 1.1GHz (3dB) electrical bandwidth, the crosstalk monotonically increases with the decrease of the channel spacing, and the crosstalk can be significant when the normalized channel spacing is lower than 2.5. This is similar to the performance observed in an analog SCM optical system [15]. Another possible approach is to use proper spectral shaping with sharp-edged filters at the transmitter to minimize the spectral overlap between adjacent subcarrier channels, and adding digital equalization at the receiver to overcome inter-symbol-interference (ISI) [16]. However, filters with large number

of taps are usually required in these systems to produce sharp edges for acceptable channel isolation, which increases the complexity in digital implementation.

It is important to note that crosstalk cancellation based on orthogonality and digital integration in the receiver requires time synchronization between digital symbols carried by adjacent SCM channels. Although phase synchronization between subcarriers may not affect system performance, misalignment between symbols carried by these channels may result in incomplete cancellation of the crosstalk [17]. Time mismatch tolerance is an important performance measure of DSCM-OFDM systems, especially if adjacent subcarrier channels originate from different optical transmitters in a distributed optical network. Figure 5(b) shows the measured BER as the function of the normalized time misalignment, where T stands for the symbol period. Since the largest crosstalk comes from adjacent channels, ch-8 and ch-9 (as indicated in inset (a) of Fig. 2) were used in this measurement, in which signal was transmitted over 75km SMF and the receiver OCNr was 1dB. Figure 5(b) indicates that the DSCM-QPSK system can tolerate the time mismatch of up to $\pm 20\%$ of symbol period without significant BER degradation. In a dynamic optical network, bit walk-off between adjacent subcarrier channels caused by fiber chromatic dispersion may change with the fiber length between the transmitter and the receiver. In our experiment with 1.11 Gbaud/s symbol rate on each subcarrier, the corresponding time misalignment tolerance is about ± 200 ps, equivalent to the differential delay of approximately 1500km of standard single mode fiber when the subcarrier channel spacing is 1.11GHz. For systems with longer fibers, digital compensation in the receiver can be applied to minimize the differential delay between channels.

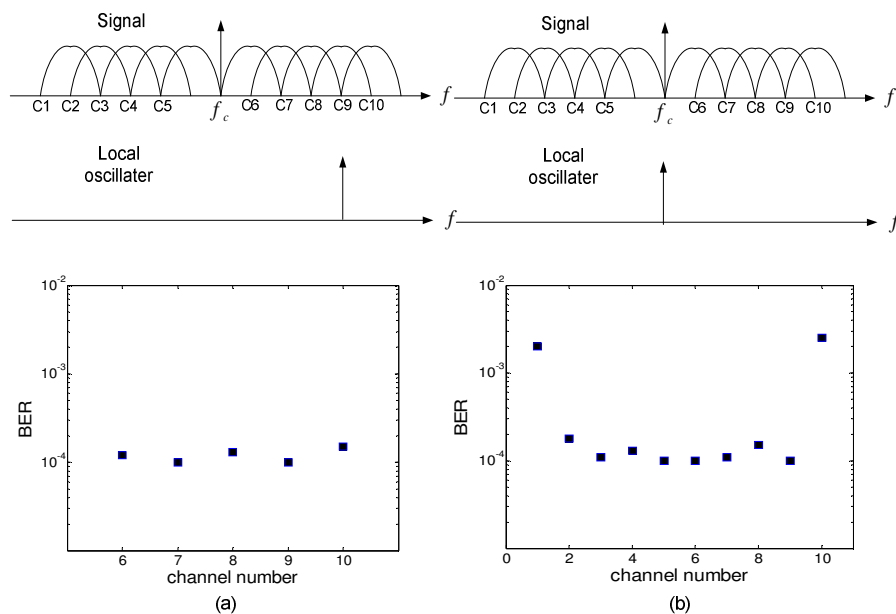


Fig. 6. BER measured as a function of the channel index for (a) when the local oscillator was tuned to channel 9, and (b) when the local oscillator was tuned to the center optical carrier.

4.3 Flexible data rate

As discussed in section 2, when higher data rate is required by an end user, multiple subcarriers can be delivered to the same end user without changing the network architecture. The end user tunes the local oscillator to one of the subcarrier frequencies in the OFDM spectrum, and coherent IQ detection translates the optical spectrum to the electrical domain with the selected subcarrier channel in the center. Then a selected number of subcarrier channels within the receiver bandwidth can be detected and recovered by digital heterodyne

detection in the receiver DSP. Note that these selected channels do not have to be adjacent to each other. In order to test this scheme, we measured the BER of selected channels in a ten channel QPSK system over 75km SMF, and with 1.5 dB OCNR at the receiver. In Fig. 6 (a) the wavelength of the local oscillator is set at subcarrier channel C9, and the BERs of five adjacent channels are measured, indicating no significant performance variation among channels. We also set the local oscillator wavelength to the center of the signal optical carrier as showed in Fig. 6 (b) in an attempt to detect all the ten subcarrier channels. The results show reasonably uniform BER performance except for the two outmost channels C1 and C10. The increased BER in these two channels is due to the bandwidth limit of the real-time oscilloscope which is 6GHz, and portions of the spectra of these two channels are already outside of this receiver bandwidth.

4.4 Fiber nonlinearity

In addition to linear degradation effects discussed above, OCNR penalty caused by fiber nonlinearity is another important parameter to be investigated in optical transport systems. Figure 7 shows the calculated OCNR penalty as the function of the optical power launched to the fiber. The simulation parameters are the same as those used to obtain Fig. 4. The simulation exams a QPSK modulated DSCM system with a fixed 20Gb/s total data rate, but partitioned into different number of subcarrier channels. The total length of standard single mode fiber was 450km divided into 6 amplified spans. If the system only has two subcarrier channels (10Gb/s per channel), there is minimum impact due to four wave mixing (FWM) and therefore OCNR penalty is relatively small. Increasing the number of subcarrier channels moderately increases the penalty due to fiber nonlinearity. But this degradation ceases to increase when the number of channels is high enough (at the same time the data rate per channel becomes low). There is no significant increase from 6 to 10 subcarrier channels as shown in Fig. 7. Therefore, from nonlinearity point of view, there is no limitation on the number of subcarrier channels that can be used in the DCSM implementation. Further reduction in OCNR penalty due to fiber nonlinearity can be realized also by forward-error correction [18].

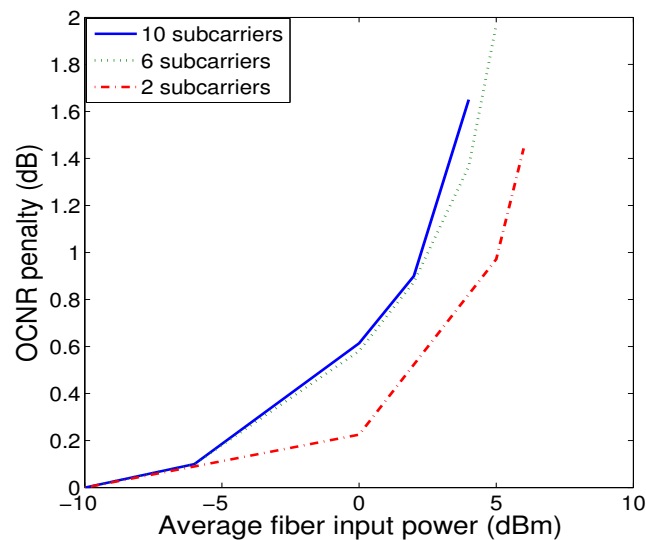


Fig. 7. OCNR penalty as a function of average fiber input power.

5. Conclusion

We have demonstrated a DSCM optical system which provides flexible bandwidth allocation and adjustable data rate granularity. In DSCM, since subcarrier channels are digitally generated in electrical domain, it allows high degree flexibility and dynamic provisioning of subcarrier channels in both data rate and power levels. We have experimentally investigated the transmission of a 22.2Gb/s DSCM-OFDM system with 10 QPSK modulated subcarrier channels over 75km single-mode fiber (SMF) without dispersion compensation. One or multiple of subcarrier channels from the optical spectrum can be recovered either individually or as a group as desired on the sub-wavelength level. Orthogonality and cancelation of crosstalk rely on the precise setting of channel spacing and the temporal synchronization of data bits between subcarrier channels. Clock synchronization has to be within $\pm 20\%$ of the symbol period to avoid significant crosstalk between subcarrier channels.